Defence Science Journal, Vol. 65, No. 5, September 2015, pp. 395-402, DOI : 10.14429/dsj.65.8725

Combined Tracking Strategy Based on Unscented Kalman Filter for Global Positioning System L2C CM/CL Signal

Xuefen Zhu[*,!], Fei Shen[*], Jianfeng Chen[#], Yang Yang[*], Dongrui Yang[*], and Xiyuan Chen[*]

[*]*Key Laboratory of Micro-Inertial Instrument and Advanced Navigation Technology of Ministry of Education, School of Instrument Science and Engineering, Southeast University, Nanjing, 210 096, China*
[#]*Automotive Engineering Research Institute, Jiangsu University, Zhenjiang, 212 013, China*
[!]*E-mail: zhuxuefen@seu.edu.cn*

ABSTRACT

In a global positioning system receiver, the tracking algorithm plays a dominant role since the code delay and Doppler frequency shift need to be accurately estimated as well as their variation over time need to be continuously updated. Combine unscented Kalman filter (UKF) with CM/CL signal to improve the signal tracking precision is proposed. It allow weighting assignment between CM code and CL code incoming signal, masked by a mass of noise, and to describe a UKF tracking loop aiming at decreasing numerical errors. UKF here involves state and measuring equations which calculate absolute offsets to adjust initial code and carrier phase then dramatically decrease the tracking error. In particular, the algorithm is implemented in both open space and jammed environment to highlight the advantages of tracking approach, by comparing single code and combined code, UKF and EKF tracking loop. It proves that signal tracking based on UKF, with low energy dissipation as well as high precision, is particularly appealing for a software receiver implementation.

Keywords: global positioning system, GPS receiver, tracking algorithm, unscented Kalman filter, CM/CL signal, weighting assignment

NOMENCLATURE

A	Amplitude of L2C signal
f_I	Frequency of the IF signal
f_d	Doppler frequency shift
ϕ_0	Initial carrier phase
t_0 and t_k	Starting and present time
$D(t)$	Navigation data
$v(t)$	White Gaussian noise
n	Sampling number of an integration
t_s	Time difference between received code and local code
δ	Time difference between early and prompt code
m	Reference index
ω_{L2}	Frequency of L2C signal
$\omega_d t_k$	Carrier phase of the receiver
B_n	Noise bandwidth of a carrier loop
C/N_0	Signal-to-noise ratio
T_1 and T_2	Navigation data period
d	Gap between two correlators
a and b	Energy of CM and CL code
X_m	State vector
X_ω	Doppler frequency difference
ΔT	Period of the CM code
G_ϕ & G_{ts}	Gaussian white noise
A_m & A_{m-1}	Carrier amplitude of index m and m-1
$\overline{A}_m$	Average carrier amplitude during 20ms
n_k	Sampling number during 1ms
$\overline{A}_k$	Average carrier amplitude
$\Delta\phi_k$	Aaverage carrier phase difference
Δt_k	Code phase difference during 1ms
k_m	First index of 20ms integration time
$\Delta\phi_m$	Average carrier phase difference
Δt_m	Average code phase difference
$A_{G_{m-1}}$	Amplitude of index $m-1$
t_{midm}	Code phase of the middle time

1. INTRODUCTION

The last decade has seen the trial sub stage of global positioning system (GPS) satellite based on L2 frequency band for civilian applications. Opening up a new band mainly aims at improving the quality of the positioning services in low signal-to-noise ratio environment since the long length code (CL code) included here can realise more precise coherent integration than C/A code or CM code[1]. So the usable signal, drowned in the noise, can be extracted thus enlarging GPS applications.

The first operation performed by GPS receiver is signal acquisition, which provides a coarse estimation of the code delay and Doppler frequency shift[2]. Then tracking procedure, mainly offers an accurate estimation and continuous update. However, L2C signal includes moderate length code (CM code) as well as long length code (CL code) which based on time division multiplexing[3]. The former is modulated by navigation data and the latter is for pilot frequency according

Received 23 April 2015, revised 16 July 2015, online published 11 September 2015

to its signal structure. In this case, conventional single code tracking inevitably wastes the other half acquired energy[4]. Meanwhile, the high-complexity and nonlinearity of the L2C signal in jammed environment reduce the tracking precision in traditional methods, since they usually adopt approximate linear filter if possible[5]. By consequence, these approaches become weak performers when facing with CL code and relatively complicated computation.

The contribution of this work is to propose a CM/CL combined signal tracking strategy that makes use of the goodness of UKF nonlinear measuring equations. We describe a UKF iterative algorithm of tracking loop to decrease tracking error of nonlinear data as well as we take the weighting assignment between CM code and CL code into consideration for maximum energy utilisation. Then prove and discuss them.

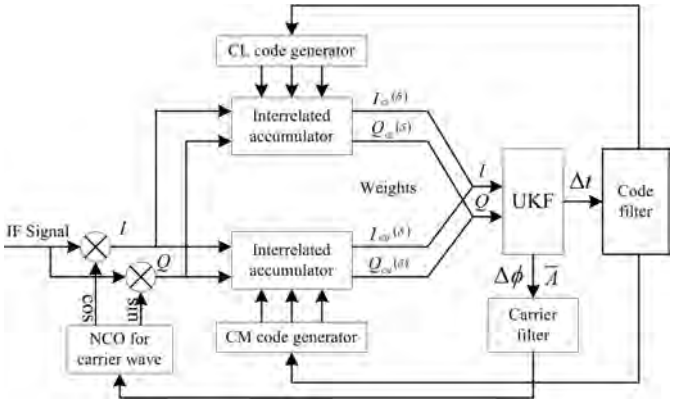

Figure 1. Combination of CM/CL code based on UKF.

2. STRATEGY OF CM/CL CODE COMBINATION

2.1 Principle of CM/CL Code Combination

In present GPS L2C signal receiver architecture, the operation of tracking mainly copies the expert model of traditional C/A code tracking, which uses single code tracking algorithm. But either single CM or single CL code, only half received energy resource is utilised because of the time division multiplexing. Meanwhile, single CM code cannot gain enough navigation information in jammed environment and single CL code needs much more time for acquisition, which increases the computational load[6]. In this context, these problems force receiver to carry out an efficient algorithm to combine advantages of both codes and to avoid the adverse factors. So, a block diagram of the combination frame is put forward in Fig. 1.

In-phase (I) and quadrature phase(Q) baseband signals are separated from the digital intermediate frequency (IF) signal. Then single CM and CL tracking loops are used to track these branches with costas or phase lock loop independently. But in the L2C signal, costas is not the most appropriate solution since its tracking result may be affected by the long integration time, about 1.5 s. After that, the weighting assignment algorithm between CM code and CL code is implemented before UKF processing. The details of signal process are shown as follows. First, the feature of incoming IF signal is:

$$y_k = A[D(t_k)CM(t_k - t_0) + CL(t_k - t_0)] \cos[2\pi(f_I + f_d)t_k + \phi_0] + v(t_k) \quad (1)$$

where A is the amplitude of L2C signal. f_I : the frequency of the IF signal; f_d : the Doppler frequency shift; ϕ_0 : the initial carrier phase; $CM(t)$:CM code with 20ms period; $CL(t)$: CL code with 1.5s period; t_0 and t_k : the starting and present time of input signal; $D(t)$:the navigation data with 20ms pulse width; $v(t)$: the white Gaussian noise. Given these parameters, the integration time of the CL code is 1.5 s, 75 times of CM code. So the CM code utilises the Costas tracking loop to track the carrier phase, while CL code need to adopt the Phase Locking Loop (PLL) to avoid accuracy loss. Specific details of tracking scheme are described in next three steps.

Step 1. Split I as well as Q signals in each time interval of the CM code and CL code. Outputs of separated signals during 20 ms[3, 4], a CM code period, are shown in Eqn (2) and CL code signal possesses the similar separated forms.

$$I_{CM}(\delta) = \sum_{k=mn}^{(m+1)n-1} y_k CM(t_k + \delta - t_s) \times \cos[(\omega_{L2} - \omega_d)t_k]$$
$$Q_{CM}(\delta) = \sum_{k=mn}^{(m+1)n-1} y_k CM(t_k + \delta - t_s) \times \sin[(\omega_{L2} - \omega_d)t_k] \quad (2)$$

where n is sampling number of an integration period, m : the reference index; Subscripts CM : CM code signal; δ : the time difference between early and prompt code; t_s : the time difference between received code and local code; ω_{L2} : the frequency of L2C signal; $\omega_d t_k$: the carrier phase of the receiver. Outputs of equation get the split value of in-phase and quadrature phase during the number m coherent integrating range, which begins at the number point and involves n points.

Step 2. Accurately estimate the code delay and Doppler frequency shift of split signals and their variations. The tracking loop is designed as a delay locked loop (DLL), which generates the prompt (P), early (E) and late (L) code as the observed value of tracking loop[7]. Figure 2 shows the structure of CM code tracking loop. CL code tracking provides a similar framework expect the PLL loop. During CM code tracking, the Fig.2 indicates the Costas discriminator applies the difference between early and late energy to adjust the initial signal until locally generated copy matches the input signal[8]. The offset

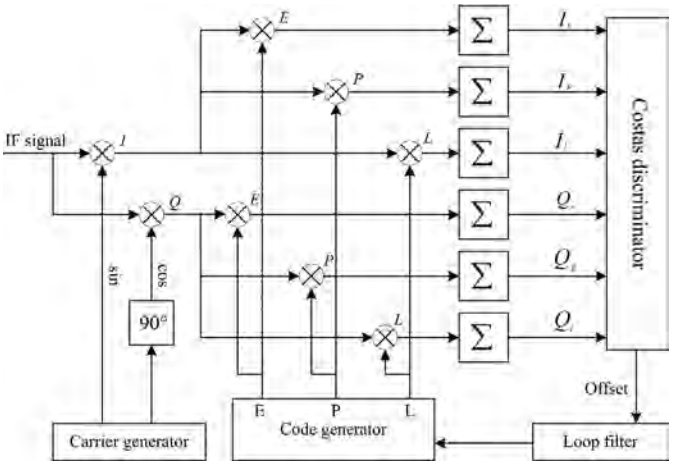

Figure 2. Frame of CM code tracking loop.

produced by the discriminator, called discrimination factor (D), is as shown in Eqn (3).

$$D = \frac{(I_e^2 + Q_e^2) - (I_l^2 + Q_l^2)}{(I_e^2 + Q_e^2) + (I_l^2 + Q_l^2)} \tag{3}$$

where I_e, Q_e are the early in-phase and quadrature phase signals and I_l, Q_l are the late signals. Then, repeat the tracking step in Step 2 until GPS receiver get maximum of I and minimum of Q, both in CM code and CL code. Unfortunately, either single CM or CL code tracking loop, mentioned above, is only for half energy utilisation since it is quite enough for tracking in an ordinary way. Meanwhile, CL code's acquisition needs much more time and computational load than CM code. However, the time-frequency dual folding technique[9], involved in our previous work, can effectively short the CL code sequence length, relax the computational burdens and make the implementation of combination algorithm possible.

Step 3. Make a combination and weighting assignment between two codes. In the conventional architecture, the methods inevitably include code and carrier phase errors, which will certainly affect tracking accuracy. These errors are related to their variance formulas, listed as follows:

$$\begin{aligned} \sigma_{\tau 1}^2 &= \frac{B_n d}{2aC/N_0}\left[1 + \frac{1}{aC/N_0 T_1}\right] \\ \sigma_{\tau 2}^2 &= \frac{B_n d}{2bC/N_0}\left[1 + \frac{1}{bC/N_0 T_2}\right] \end{aligned} \tag{4}$$

where B_n is the noise bandwidth of a carrier loop. C/N_0: the signal-to-noise ratio; T_1 = 20 ms and T_2 = 1.5 s: navigation data period; d : the gap between two correlators; a = 0.5: the energy share of CM code; b also equals 0.5 meaning the occupied energy of CL code. Then a weighting assignment strategy is taken into consideration for combination in this paper according to Tran[10], *et al.*. When weighting parameters $\alpha = \sigma_{\tau 2}^2 / (\sigma_{\tau 1}^2 + \sigma_{\tau 2}^2)$ and $\beta = \sigma_{\tau 1}^2 / (\sigma_{\tau 1}^2 + \sigma_{\tau 2}^2)$, the code phase variances will get minimum value. Last but most important operation is to allocate I and Q phase signals between CM code and CL code tracking loop. It means that Q_X and I_X in Step 2 are replaced by $I_Y = \alpha I_{CM} + \beta I_{CL}$ and $Q_Y = \alpha Q_{CM} + \beta Q_{CL}$ each iteration. Easy to find that the tracking strategy in Step 2 is a special case if one of weight parameters (α or β) here is set as zero.

3. DESIGN OF UKF ALGORITHM

3.1 Principle of UKF Tracking Loop

The unscented Kalman filter (UKF), suggested by Julier and Uhlman, has become a popular alternative to the extended Kalman filter (EKF) during the last decade[13]. Although the modified EKF algorithm[12, 13] improves the accuracy of tracking loop, their tracking error in low signal to noise ratio is not ignorable. And although UKF[14] has been involved in GPS signal tracking, its signal-to-noise ratio is limited as 27 dbHz because of the improper mathematical model. In addition, these methods just applied UKF in GPS L1 signal. So a block diagram representation of UKF application is presented in this paper, as shown in Fig.1. During each iteration stage, it is used to adjust the feedbacks I and Q phase signal thus improving tracking accuracy. UKF tracking loop estimates as well as updates code phase and carrier frequency by observing the value of I_e, Q_e, I_l, Q_l, and I_p, Q_p at the same time for building state and measuring equation. The state equations based on choosing state quantities, as shown in Eqn (5), are seen as the index state of incoming $I(\delta)$ and $Q(\delta)$ signal above.

$$X_m = [(X_\phi)_m \;\; (X_\omega)_m \;\; (t_s)_m \;\; A_m]^T \tag{5}$$

X_m is the state vector which includes four state quantities. where X_ϕ: the difference between input and local carrier phase; X_ω : the Doppler frequency difference; t_s : the difference between input and local code phase; A_m : the carrier amplitude; m: the reference index. Then four state equations, reflecting the transformation relation between the reference index m and, m-1, are listed as follows:

$$\begin{aligned} &\begin{bmatrix} X_\phi \\ X_\omega \end{bmatrix} = \begin{bmatrix} 1 & \Delta T \\ 0 & 1 \end{bmatrix} \begin{bmatrix} X_\phi \\ X_\omega \end{bmatrix}_{m-1} + \begin{bmatrix} 1 & 0 \\ 0 & 1 \end{bmatrix} \begin{bmatrix} G_\phi \end{bmatrix}_{m-1} \\ &(t_s)_m = (t_s)_{m-1} + \frac{\omega_{L2}\Delta T - \begin{bmatrix} 1 & 0 \end{bmatrix} \begin{bmatrix} G_\phi \end{bmatrix}_{m-1}}{\omega_{L2} + (X_\omega)_{m-1}} + (G_{ts})_{m-1} \\ &A_m = A_{m-1} + A_{G_{m-1}} \end{aligned} \tag{6}$$

where ΔT is 20 ms, which chooses the period of the CM code since it is shorter than the CL code; G_ϕ and G_{ts} : the Gaussian white noise. ω_{L2} : the frequency of the L2C signal; A_m and A_{m-1} : carrier amplitude of index m and $m-1$; $A_{G_{m-1}}$: the amplitude of index $m-1$ white noise sequence. These equations reflect the change of state quantities with time (or index number). As is shown in Step 2 in last section, the discriminator utilises the difference between early and late energy to adjust initial signal until matching with each other. The measuring equation, a 4x1 matrix whose first two lines reflect the prompt carrier phase ($\delta = 0$) and last two lines reflect the difference between early and late carrier phase, will be built next. Here $I_k(\delta)$ and $Q_k(\delta)$ can be expressed as follows:

$$\begin{aligned} I_k(\delta) &= \frac{1}{2} n_k \bar{A}_k D_k \cos(\Delta\phi_k) R(\Delta t_k + \delta) + v_{Ik} \\ Q_k(\delta) &= \frac{1}{2} n_k \bar{A}_k D_k \sin(\Delta\phi_k) R(\Delta t_k + \delta) + v_{Qk} \end{aligned} \tag{7}$$

where n_k is the sampling number during 1 ms; D_k : the navigation data; $\bar{A}_k$: the average carrier amplitude, $\Delta\phi_k$: the average carrier phase difference and Δt_k : the code phase difference during 1 ms; $R(t)$: the correlation function; v_{Ik} and v_{Qk} :the uncorrelated white Gaussian noise sequences with $n\sigma_v^2/2$ variance as well as zero-mean. So the measuring equation is as shown in Eqn (8).

$$Z_m = \begin{bmatrix} \sum_{k=k_m}^{k_m+19} I_k(0) \\ \sum_{k=k_m}^{k_m+19} Q_k(0) \\ \sum_{k=k_m}^{k_m+19} [I_k(\delta) - I_k(-\delta)] \\ \sum_{k=k_m}^{k_m+19} [Q_k(\delta) - Q_k(-\delta)] \end{bmatrix} = \frac{N\bar{A}_m D_m}{2} \begin{bmatrix} \cos(\Delta\phi_m) R(\Delta t_m) \\ \sin(\Delta\phi_m) R(\Delta t_m) \\ \cos(\Delta\phi_m) R_e(\Delta t_m) \\ \sin(\Delta\phi_m) R_e(\Delta t_m) \end{bmatrix} + v_m \tag{8}$$

$$(N=\sum_{k=k_m}^{k_m+19} n_k; D_m=[D_{k_m}, D_{k_m+1},..., D_{k_m+19}];$$
$$R_e(\Delta t)=R(\Delta t+\delta)-R(\Delta t-\delta);)$$

where k_m is the first index of 20 ms integration time; $R_e(\Delta t)$: the correlated difference between early and late signal. v_m: the white Gaussian noise sequence. After initial $\Delta\phi_k$ Δt_k and $\bar{A}_k$ by least square, the value $\Delta\phi_m$: the average carrier phase difference. Δt_m: the average code phase difference and $\bar{A}_m$: the average carrier amplitude during 20ms, can be inferred by Eqn (5):

$$\Delta\phi_m=\begin{bmatrix}1 & \frac{\Delta T}{2}\end{bmatrix}\begin{bmatrix}X_\phi\\ X_\omega\end{bmatrix}_m+[0 \quad 1][G_\phi]_m$$
$$\Delta t_m=\frac{(t_s)_m+(t_s)_{m-1}}{2}-t_{midm} \tag{9}$$
$$\bar{A}_m=\frac{1}{2}(A_m+A_{m-1})$$

where t_{midm} is the code phase of the middle integration time. In Eqn (8), we define a function $h(\Delta\phi_m, \Delta t_m, \bar{A}_m)=\frac{N\bar{A}_m}{2}\begin{bmatrix}\cos(\Delta\phi_m)R(\Delta t_m)\\ \sin(\Delta\phi_m)R(\Delta t_m)\\ \cos(\Delta\phi_m)R_e(\Delta t_m)\\ \sin(\Delta\phi_m)R_e(\Delta t_m)\end{bmatrix}$, so the measuring equation can be expressed as:

$$Z_m=D_m h(\Delta\phi_m, \Delta t_m, \bar{A}_m)+v_m \tag{10}$$

According to the state equations as well as the measuring equation, the $\Delta\phi_m$, Δt, and $\bar{A}$ above can be obtained from UKF block diagram to offset the input in-phase and quadrature phase signal in each iteration during last combination algorithm to decrease tracking errors, as shown in Fig. 1. Fortunately, experiments will prove the accuracy superiority of UKF application next section.

4. SIMULATION AND DISCUSSION

4.1 CM/CL Code Combination Discussion

Both energy utilisation and accuracy play important roles in tracking of GPS receiver. Considering the single CL code acquisition need much more time and higher computational complexity, we employ the time-frequency dual folding algorithm, our previous study achievement, in signal acquisition. Necessary parameters during both acquisition and tracking are list as follows: 1) Sampling frequency f_s = 10 MHz; 2) Center frequency f_c = 2.5 MHz; 3) Pseudo code rate r_{IF} = 1.023 MHz; 4) Down-conversion multiple k_f of CL code signal; 5) The amount groups k_g of CL code signal. Figure 3 shows the acquisition results of single CM code and CL code of No. 5 satellite in open space and jammed environment. Where $k_f=6, k_g=3$ means 'down-conversion multiple is 6' and 'the amount groups is 3' in time-frequency dual folding algorithm, thus the effective code length of CL code becomes 1/18. From Fig. 3, we notice that both CM code and CL code

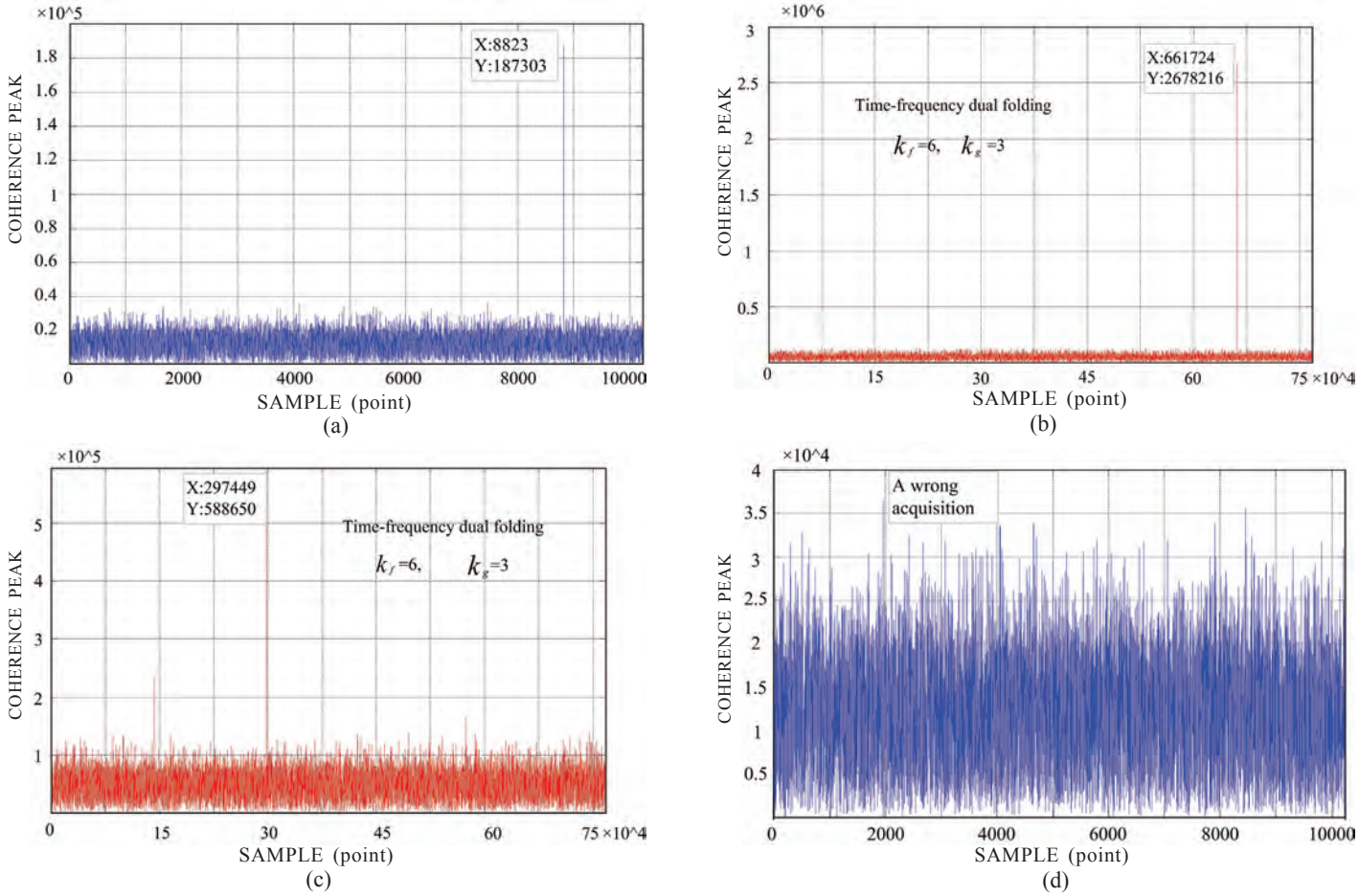

Figure 3. Correlation function of CM/CL code of No. 5 satellite (a) CM code acquisition with 46.3 dbHz, (b) CL code acquisition with 46.3 dbHz, (c) CM code acquisition with 18.9 dbHz, and (d) CL code acquisition with 18.9 dbHz.

can provide an effective coarse estimation of the code delay and the Doppler frequency shift in open space. However, when in low signal-to-noise ratio environment, the former produces a wrong acquisition result, which proves the necessity of CL code involved in jammed environment.

Unfortunately, if we change the signal energy in the test above (18.9 dbHz) through cutting down amplitude of input signal, the acquisition performance will change and lead to the instability of receiver effects. The statistical results of each 100 tests in different attenuation multiples are shown in Fig. 4, with single CL code and combination algorithm. It shows that property of CL code acquisition begin to decline when the energy attenuation multiple drops to 0.34 (the point 2). However, the degenerative point is 0.22 (the point 4) in combination algorithm. Meanwhile, the error of the latter is smaller in the whole curve as well, especially between the attenuation areas of two, which proves the superiority of combination of CL and CM code in low signal-to-noise ratio, low-energy area, such as an indoor environment.

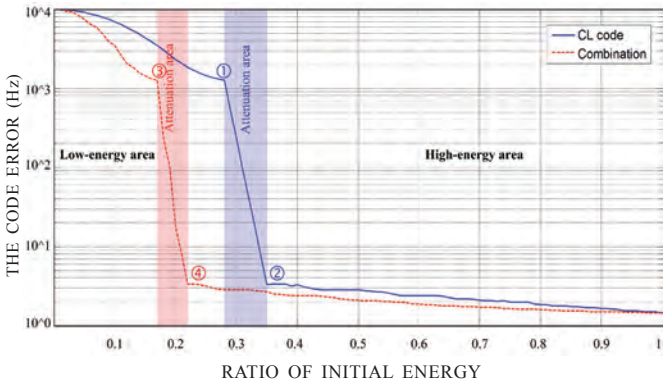

Figure 4. The relation between code error and energy attenuation.

During combination, the weighting parameters α and β are obtained according to the variance of the CM code phase and CL code phase when make a combination tracking, which is expressed as follows:

$$\frac{\alpha}{\beta}=\frac{\sigma_{\tau 2}^2}{\sigma_{\tau 1}^2}=\frac{1+1/[b(C/N_0)T_2]}{1+1/[a(C/N_0)T_1]} \tag{11}$$

where $a=b=0.5$; $T_1=0.02s$; $T_2=1.5s$; and $C/N_0=18.9dbHz$. So, $\alpha=0.146$ and $\beta=0.854$ in each tracking iteration. Figure 5 gives the tracking results of single CL code and the UKF combination algorithm, which includes 400 ms frequency tracking and 800 ms phase tracking. It shows that the subtle signal jitter of combination algorithm is smaller than CL code tracking, proving the better stability. And that a rough estimation of computational complexity of single CL code and combination is $C_{CL}:C_{C0m}=1:1.06$, indicating the approximate computational burdens. This test result means the higher accuracy and twice energy utilisation get in return at the cost of a few computational loads.

During the 400 ms frequency tracking scheme, the ratio A_{ca}/P_{ca} between amplitude of the carrier phase error and carrier period is used for evaluating the carrier tracking performance of tracking models above. The

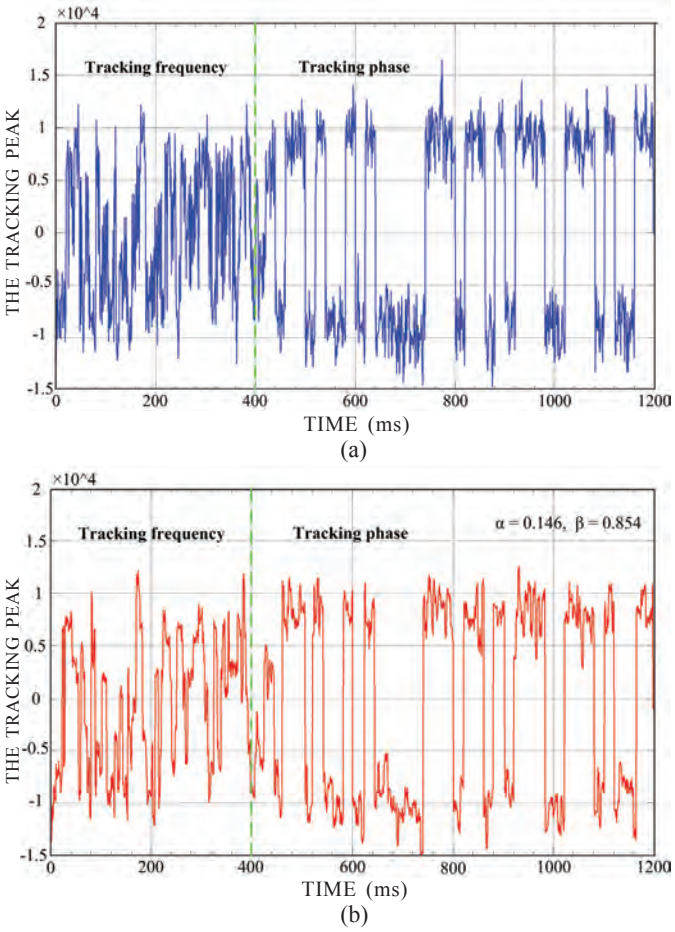

Figure 5. The tracking results of single CL code and combination (a) CL code tracking and (b) UKF combination tracking.

carrier phase error curves, tested in different signal-to-noise ratio environments (choosing six places) are shown in Table 1. It clearly indicates that the choice of code has a great influence in carrier frequency tracking effects, even all models based on UKF algorithm. It is easy to find that carrier errors of three are similar when in high signal-to-noise ratio environment. But the speed of CM code tracking degradation is much faster than other two models if the signal-to-noise ratio begins to decline. According to the average degradation speed, the combination strategy improves the performance of frequency tracking about 32.6 per cent by single CM code and about 2.4 per cent by single CL code as a whole.

In addition, Fig. 6 shows the carrier error curves of single CM code and combination of both in 18.9 dbHz, which shows that the error is -5~5 chips and -2.5~2.5 chips, proves the superiority of combination algorithm.

Table 1. The carrier phase error statistics of models

	(Hz)	18.9	25.6	30.4	44.5	46.3	53.1
A_{cd}/P_{ca} based on UKF	CM code	0.235	0.198	0.126	0.064	0.056	0.050
	CL code	0.133	0.129	0.082	0.054	0.055	0.050
	Combination	0.132	0.124	0.078	0.055	0.054	0.048

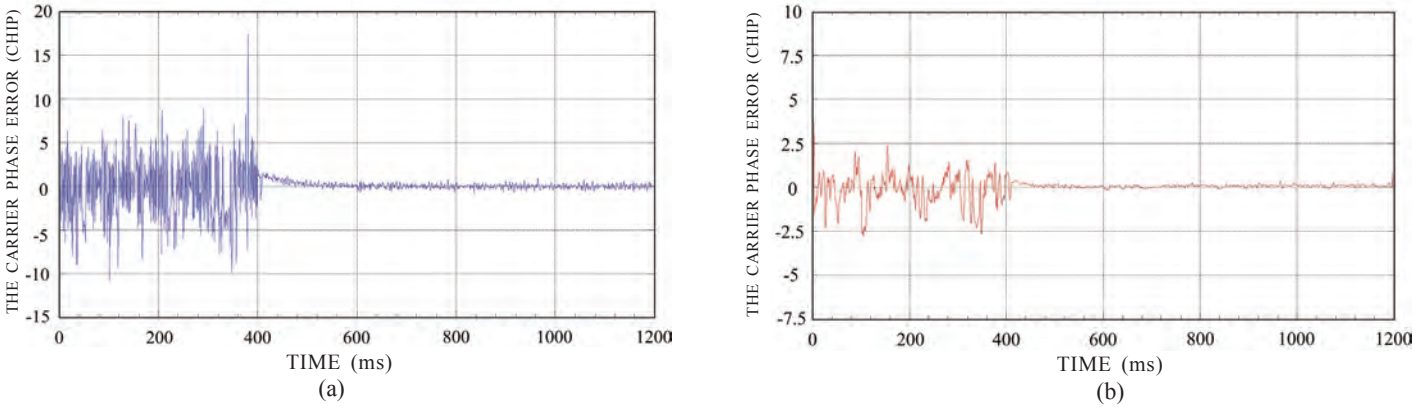

Figure 6. The carrier phase error curves (18.9dbHz) (a) CM code tracking and (b) UKF combination tracking.

4.2 Performance Analysis of UKF Algorithm

During the 800 ms code phase tracking scheme, to prove the effectiveness of UKF algorithm, Fig. 7 gives the code errors of tracking loop with and without UKF in 18.9 dbHz as well as 46.3 dbHz environments. These curves clearly show that UKF design improves the tracking performance tremendously. The maximal code phase error of traditional tracking loop is more than chips; nevertheless, it is limited in $-0.1 \sim 0.2$ chips with UKF algorithm in jammed environment. And in 46.3 dbHz signal-to-noise ratio area the code error of UKF is much smaller as well, which is limited in $-0.01 \sim 0.035$ chips.

Meanwhile, the standard deviations of algorithms are analysed and compared in Table 2, in terms of the experiment results of Fig. 7. The table highlights the advantages of UKF method compared to the conventional pure tracking loop since the error standard deviation of the latter is 13.3 and 5.5 times of the former in open and jammed environment.

Table 2. The standard deviations of code phase error

Standard deviation (chip)	Traditional algorithm	UKF algorithm
18.9 dbHz	0.34	6.2×10^{-2}
46.3 dbHz	6.8×10^{-2}	5.1×10^{-3}

In particular, we compared the EKF and UKF design strategy of L2C signal receiver. Both in EKF and UKF method, necessary parameters initialised listed one as follows:

(a) Bandwidth of DLL loop filter

(b) Coherence interval of CM code and CL Code

(c) Interval time of EKF and UKF tracking loop

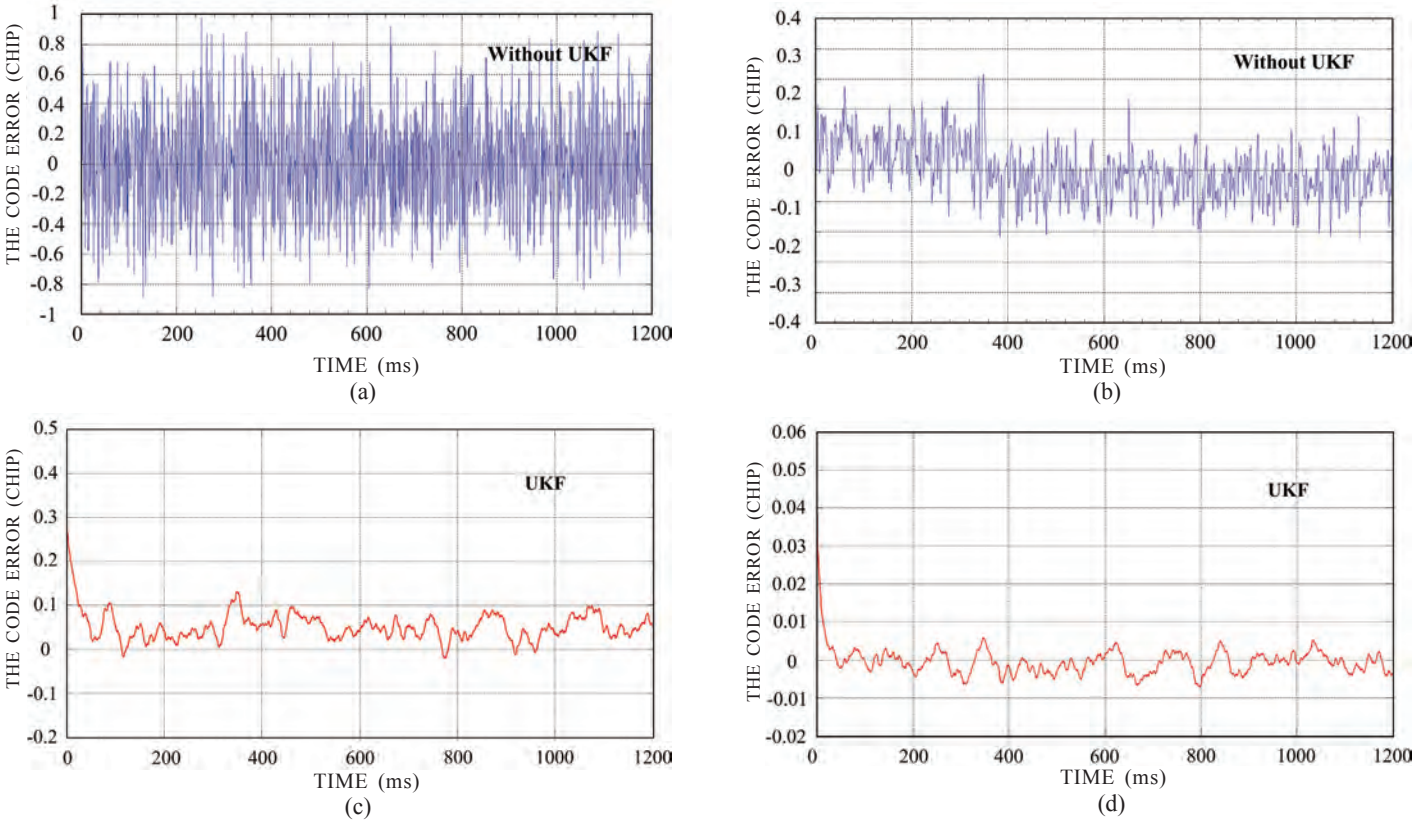

Figure 7. The code error curves of different and models (a) 18.9 dbHz without UKF process, (b) 46.3 dbHz without UKF process, (c) 18.9 dbHz with UKF process, and (d) 46.3 dbHz with UKF process.

(d) Bandwidth of PLL loop filter
(e) Decay factor of PLL loop.

The difference of both is that UKF uses the statistical property while EKF is inclined to utilise the Jacobian matrix and partial differential algorithm for signal estimation[11]. So, viewed from the algorithm theory, the UKF tends to be more accurate in high-complexity and nonlinearity signal application. Figure 8 shows the Doppler frequency shift curves of EKF and UKF in 18.9 dbHz environment. It can be seen that the fluctuation of EKF is large than UKF, indicating that the UKF tracking loop is more stable. Meanwhile, proposed UKF strategy needs lesser time to convergence than EKF tracking loop. Moreover, UKF and EKF algorithms are both three orders, but the computational complexity of EKF is larger than UKF because of its complicated Jacobian matrix estimation. So, UKF tracking loop is more suitable in GPS L2C signal tracking.

To sum up, experiments above prove that the tracking based on UKF for GPS L2C CM/CL combined signal is effective, with relatively high accuracy, energy utilisation and relatively relaxed computational load, which is particularly appealing for a GPS software receiver implementation. Although it is more suitable in jamming environment, the larger computation load of UKF tracking loop than that without UKF make it become unnecessary and redundant in open space.

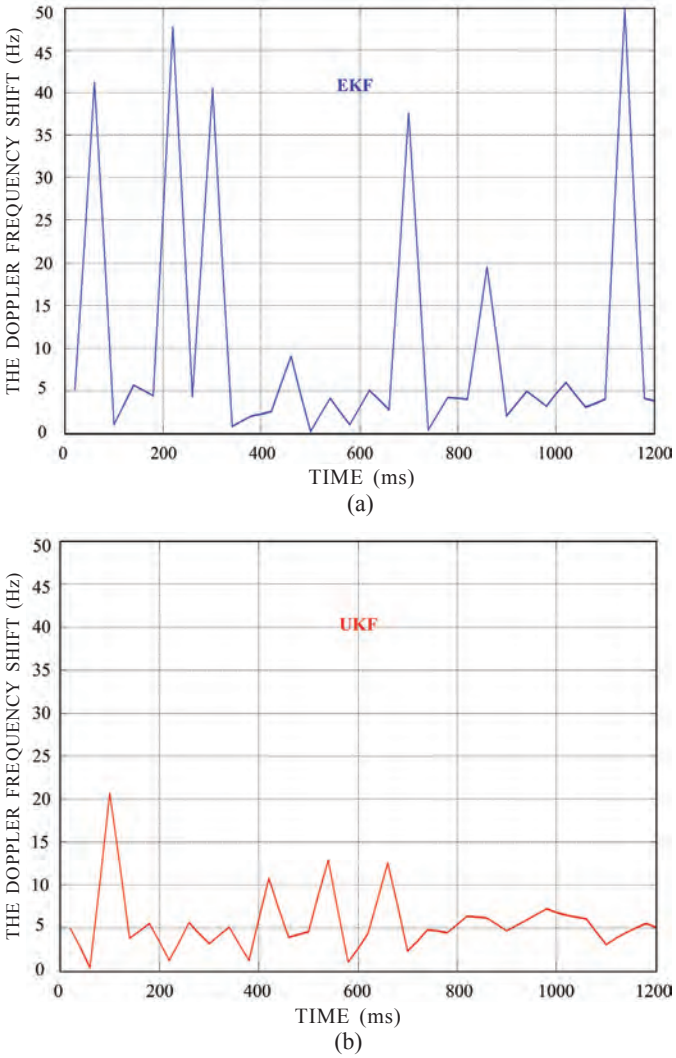

Figure 8. The Doppler frequency shift curves (18.9 dbHz): (a) EKF tracking loop and (b) UKF tracking loop.

5. CONCLUSION

The strategy of CM and CL code combination based on UKF, proposed, provides an efficient means of GPS L2C signal application in low signal-to-noise ratio environment. Combination of codes improves the energy utilisation by 50 per cent, which plays an important role in weak signal area. During the combination algorithm, the operation of weighting assignment between CM code and CL code is to obtain minimal code and carrier errors. Meanwhile, the UKF tracking loop dramatically decreases the code and carrier phase error as well as increases signal tracking accuracy. Experiments in both open space and jammed area demonstrate the stability of described approach, by comparing single code and combined code tracking, UKF and EKF tracking loop.

REFERENCES

1. Lei, J.-F. & Will, H. A. Thin-film thermocouples and strain-gauge technologies for engine applications. *Sens. Actuators A.*, 1998, **65**(2-3), 187-193. doi: 10.1016/S0924-4247(97)01683-X
2. Martin, L.C.; Fralick, G.C. & Taylor, K.F. Advances in thin film thermocouple durability under high temperature and pressure testing conditions: National Aeronautics and Space Administration. Lewis Research Center, 1999.
3. Grant, H.; Przybyszewski, J. & Claing, R. Turbine blade temperature measurements using thin film temperature sensors. Pratt and Whitney Aircraft, East Hartford, CT (USA)1981.
4. Martin, L.C. & Holanda, R. Applications of thin-film thermocouples for surface temperature measurement. *In* SPIE's 1994 International Symposium on Optics, Imaging and Instrumentation, 1994, pp. 65-76.
5. Parvis, M.; Grassini, S. & Barresi, A. Sputtered thermocouple for lyophilization monitoring. *In* Instrumentation and Measurement Technology Conference (I2MTC), 2012 IEEE International, 2012, pp. 1994-1998. doi: 10.1109/i2mtc.2012.6229263
6. Matsuki, K.; Narumi, R.; Azuma, T.; Yoshinaka, K.; Sasaki, A. & Okita, K. Temperature distributions measurement of high intensity focused ultrasound using a thin-film thermocouple array and estimation of thermal error caused by viscous heating. *In* Engineering in Medicine and Biology Society (EMBC), 2013 35th Annual International Conference of the IEEE, 2013, pp. 3722-3725. doi: 10.1109/embc.2013.6610352
7. Varrenti, A.R.; Zhou, C.; Klock, A.; Chyung, S.H.; Long, J. & Memik, S.O. Thermal sensing with lithographically patterned bimetallic thin-film thermocouples. *Electron Device Lett., IEEE*, 2011, **32**, 818-820. doi: 10.1109/LED.2011.2136314
8. Sarma, U. & Boruah, P.K. Design and development of a high precision thermocouple based smart industrial

thermometer with on line linearisation and data logging feature. *Measurement*, 2010, **43**(10), 1589-1594. doi: 10.1016/j.measurement.2010.09.003

9. Wrbanek, J.D.; Fralick, G.C. & Zhu, D. Ceramic thin film thermocouples for SiC-based ceramic matrix composites. *Thin Solid Films*, 2012, **520**(17), 5801-5806. doi: 10.1016/j.tsf.2012.04.034
10. Lassner, E. & Schubert, W.-D. Tungsten: properties, chemistry, technology of the elements. Alloys, and Chemical Compounds: Springer, 1999. doi: 10.1007/978-1-4615-4907-9
11. Lei, J.-F.; Kiser, J.D.; Singh, M.; Cuy, M.; Blaha, C.A. & Androjna, D. Durability Evaluation of a Thin Film Sensor System With Enhanced Lead Wire Attachments on SiC/SiC Ceramic Matrix Composites. NASA TM—2000-209917, March 2000.
12. Bechtold, T.; Rudnyi, E.B. & Korvink, J.G. Fast simulation of electro-thermal mems: Efficient dynamic compact models. Springer, 2007.
13. Ebling, D.; Jaegle, M.; Bartel, M.; Jacquot, A. & Böttner, H. Multiphysics simulation of thermoelectric systems for comparison with experimental device performance. *J. Electron. Mater.,* 2009, **38**(7), 1456-1461. doi: 10.1007/s11664-009-0825-0
14. Antonova, E.E. & Looman, D.C. Finite elements for thermoelectric device analysis in ANSYS, *In* 24th International Conference on Thermoelectrics, 2005, pp. 215-218. doi: 10.1109/ict.2005.1519922

ACKNOWLEDGMENTS

The project is supported by National Natural Science Foundation of China (41104015 and 51405203) and Jiangsu Overseas Research and Training Program for University Prominent Young and Middle-aged Teachers and Presidents. We would like to thank these institutions for the funding help. We also thank Dr Xu Yuan of School of Instrument Science and Engineering of Southeast University for his helpful suggestions.

CONTRIBUTORS

Dr Xuefen Zhu received a PhD in Navigation, guidance and control engineering in 2010, at Southeast University, China. Since April 2013 she has been Associate Professor in the school of Instrument Science and Engineering of Southeast University. Her research activities are focused on GNSS signal processing and GNSS/INS integration technologies.

Mr Fei Shen is a master's candidate of Southeast University, China. His research activities are focused on advanced signal processing and fault diagnosis field.

Mr Jianfeng Chen received his Master's degree from Jiangsu University in 2005. He is now a PhD student at Southeast University. He is also a Lecturer with Jiangsu University. His current research interests include inertial navigation and SINS/GNSS integrated measurement.

Mr Yang Yang is now a master student at Southeast University. His research focuses on GPS/Galileo software receivers and integrated navigation.

Mr Dongrui Yang is now a PhD student at Southeast University. His research includes GPS signal processing and inertial navigation.

Dr Xiyuan Chen received his PhD from Southeast University in 1998. He is a Professor of the School of Instrument Science and Engineering at Southeast University. His research areas include GPS software receiver, inertial navigation, wireless location technology, integrated navigation and related application.